Error Characteristics of the SIR Resolution Enhancement Algorithm

David S. Early and David G. Long
Brigham Young University
459 CB, Provo, UT 84602
801-378-4884, FAX: 801-378-6586, e-mail: earlyd@newt.ee.byu.edu

Abstract: To improve the utility of the scatterometer for land and ice studies, the Scatterometer Image Reconstruction (SIR) resolution enhancement algorithm has been developed to exploit the frequent overlapping coverage provided by the scatterometer. In this paper, we examine the effects of feature motion on SIR imagery and show the similarity of SIR motion imagery to low pass filtered truth images. Also, resolution improvement is qualified by examining radiometric accuracy as a function of spatial frequency. The SIR algorithm applied to ERS-1 scatterometer data provides a 33% gain in radiometric accuracy when compared to simple image reconstruction of raw scatterometer data.

INTRODUCTION

Spaceborne scatterometers are currently used to monitor and study near surface ocean winds on a global scale. The temporal and spatial resolution of the scatterometer make it a useful instrument for studying these atmospheric processes. Recently, the scatterometer has also been used to study non-ocean surface conditions (e.g. [1] [2] [3]). However, while the temporal coverage of the scatterometer is good for rapid repeat coverage of the Earth's surface, the nominal spatial resolution of 50 km is inadequate for detailed classification of non-ocean surface conditions.

In order to improve the resolution of the scatterometer data, a resolution enhancement technique has been developed to exploit the frequent, overlapping coverage of the spaceborne scatterometer [4]. The Scatterometer Image Reconstruction (SIR) algorithm is particularly useful for polar ice studies because of the high temporal and spatial coverage provided by scatterometers, and in fact the algorithm has been applied successfully to Seasat scatterometer data over Greenland glacial ice in [3]. It can also be used with ERS-1 data.

ERS-1 AND SIR

The ERS-1 scatterometer measurements are delivered on a 25 km grid of cells or resolution elements for each orbit. Each cell has cos^2 response as illustrated in Fig. 1 which is a result of averaging several discrete pulses into a single reading. The general effect of this averaging is a low pass filter on the collected data. The high frequency loss is accentuated by the fact that the ERS-1 roll off function extends to a radius of nearly 50km, larger than the nominal 25 km grid spacing.

SIR attempts to recover as much of the frequency information as possible from the scatterometer data stream. By using several days worth of data, multiple overlapping cells are algebraically recombined in a weighted iterative process. Resolution enhancement is achieved by backprojecting the data onto a higher resolution grid. The achievable enhancement is determined in part by the overlap characteristics of the cells and the cell shape. Seasat data, for instance, can be enhanced to greater resolution than ERS-1 data because the cell shape is oblong, resulting in a higher spatial sampling in one direction. Recombination of several days of data with various cell orientations results in a greater resolution enhancement than is possible with the larger, circular ERS-1 cell shapes. However, SIR does provide resolution enhancement to increase the use and applicability of ERS-1 data over land and ice.

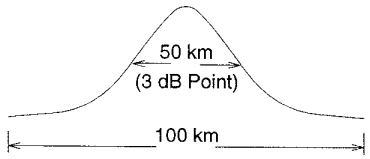

Figure 1: Geometry of the ERS-1 Footprint. Each measurement cell has a latitude and longitude that specify the center of the cell. The σ^o is assumed to have a cosine-squared roll off characteristic, with the 3 dB point at 50km. (Personal Communication, E. Attema)

This paper addresses the issue of radiometric and frequency error in the SIR algorithm for ERS-1 data. Because SIR was originally developed for use over the Amazon where microwave signatures are relatively stable over periods of days, there is a need to characterize the behavior of the algorithm over the more dynamic polar ice regions. For brevity, we consider only the simple characterization of the SIR algorithm as a low pass filter for surfaces in motion and radiometric accuracy of SIR compared to nominal ERS-1 resolution.

METHODOLOGY

Simulated data is used to characterize the SIR imagery. High resolution test scenes are processed using cell location, azimuth and incidence angle information extracted from actual ERS-1 scatterometer data. The cell response shown in Fig. 1 is used in calculating the simulated σ^o values. For the purposes of this simulation, we assume that this response is exact and that there is no location error in the latitude and longitude extracted from the actual ERS-1 data.

We model σ^o as a linear function of incidence angle:

$$\sigma^o_{dB} = \mathcal{A} + \mathcal{B}(\theta - 40°) \quad (1)$$

0-7803-3068-4/96$5.00©1996 IEEE

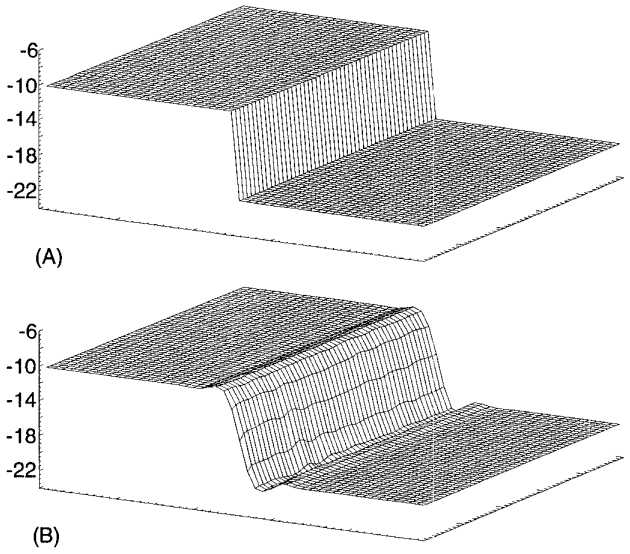

Figure 2: Example test image and SIR output. Plot (A) is the original single step image. Plot (B) is the output of SIR.

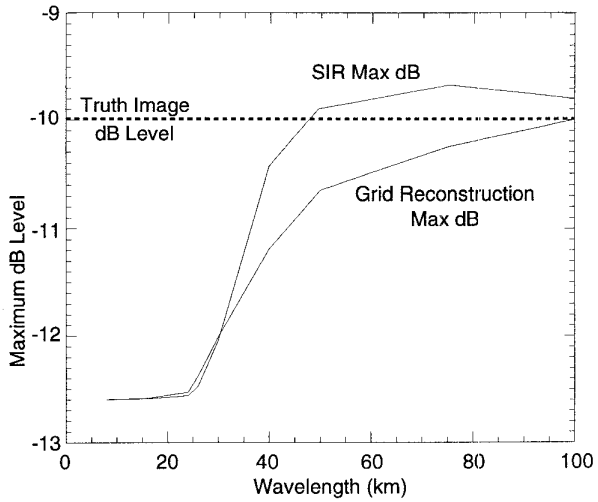

Figure 3: Convergence of the maximum dB levels for the SIR algorithm and a simple single pass reconstruction. Note SIR becomes more accurate relative to the true dB level faster than the simple grid reconstruction even with the overshoot.

where θ has been normalized to 40°, the median incidence angle in the data. Each test scene consists of two colocated images: an $\mathcal{A}$ image and a $\mathcal{B}$ image. In this study, the test scenes are at 1 km/pixel resolution. For any given cell measurement, we assume that the incidence angle is identical for each pixel in the footprint. For each pixel, the σ^o value for that pixel is calculated based on the $\mathcal{A}$ and $\mathcal{B}$ values from the test images and the incidence angle associated with the cell using (1). The cos^2 weighting function is applied and the weighted average of the pixels within a footprint represent a linear estimate of σ^o for the test 'surface'.

The simulated data stream is then processed with SIR. Surface plots of sample input and output image are shown in Fig. 2. The test scenes used in this study are two-level scenes as illustrated in Fig. 2(A). Step sizes vary from 2 dB to 20 dB, but the results for various step sizes have negligible differences.

A total of 5 days of location, azimuth and incidence data are extracted from the ERS-1 data set. Motion scenes are created using five $\mathcal{A}$ and $\mathcal{B}$ image sets, one for each day. The scenes are considered stationary over each day period. Motions of 2 km/day, 5 km/day, 10 km/day, 15 km/day and 30 km/day are considered, although a sustained speed of 30 km/day in sea ice is unlikely.

Comparison images

Comparison of SIR imagery to low pass filtered versions of the original high resolution imagery is used to assess the SIR algorithm performance. Each test scene in this study is low pass filtered to create a 'truth' image for comparison with the SIR output. The low pass filter used to create comparison 'truth' images is ideal with a spatial cutoff frequency equivalent to the resolution of the SIR imagery. For motion over multiple days, each day's image is low pass filtered and the truth image is created by averaging the individually filtered daily images.

RESULTS

Because the ERS-1 footprint extends beyond the nominal 25km grid spacing (approximately a 100 km diameter circle), significant reduction of the spatial frequency content of the original image is expected at wavelengths less than 100km. The SIR algorithm enhances the frequency content and results in a reconstructed image that is accurate at higher spatial frequencies than the nominal data provides. This is illustrated in Fig. 3. The SIR image converges to within 0.5dB of the true dB level at wavelengths of around 40km, although there is a slight overshoot. The idealized data does not reach this level of accuracy for wavelengths less than about 60km.

We note that the shape and size of the ERS-1 footprint severely limits the resolution enhancement achievable by the SIR algorithm. In a previous study using Seasat, SIR achieved a much greater resolution enhancement because of the shape and distribution of the scatterometer measurement cells [5]. It is expected that SIR will perform similarly well using NSCAT data.

Motion

Fig. 4 shows profile comparisons of SIR imagery with the low pass 'truth' images. Note that as the magnitude of the motion increases, the overshoot and undershoot of the truth images are reduced by the averaging of the individually filtered day images, but that the transition region between the high and low dB levels is the same for both SIR and the low pass truth

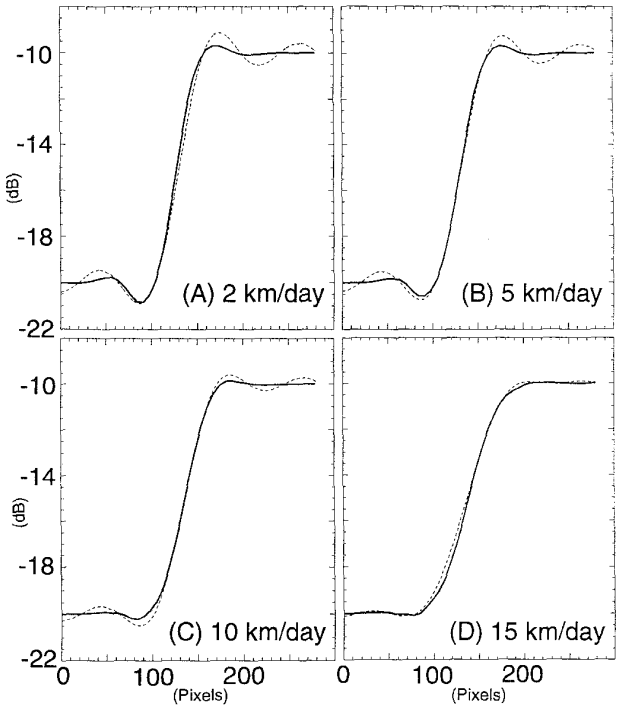

Figure 4: Cross sections of several motion examples. The solid lines are SIR image profiles, the dotted lines are low pass filtered truth image profiles.

images. Also note that the SIR images have less over- and undershoot and ripple than the low pass truth images.

Figs. 5(A) and 5(B) show a comparison of 15 km/day motion and 30 km/day motion. The ripples in the 30 km/day transition region are because the scatterometer passes over the regions at various ascending and descending angles which result in unique distributions of overlapping cells in any given scene. Because SIR uses multiple overlapping cells to reconstruct the images, areas in a scene that have limited or reduced cell coverage may not be as accurately reconstructed. In Fig. 5(A), where the underlying motion is more reasonable, the textural anomalies in the transition region are less significant.

SUMMARY

The ability of the SIR reconstruction algorithm to create accurate images at higher spatial frequencies is illustrated. SIR provides more accurate dB estimates at lower wavelengths resulting in an approximately 33% resolution gain for errors less than 0.5 dB when compared to simple grid reconstructions even with the severe limitations of the ERS-1 cell response. The SIR algorithm also produces images of stationary scenes and scenes in motion that are similar to low pass filtered versions of the original scenes allowing the algorithm to be characterized as a low pass filter. Because of the non-linearities of the SIR algorithm, the overshoot and undershoot characteristic of low pass filtering are reduced in SIR imagery. This suggests that SIR is more effective than simple construction of imagery from raw ERS-1 scatterometer data.

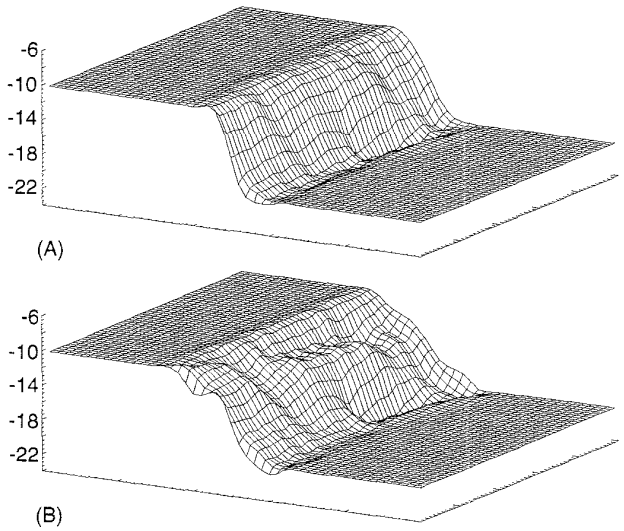

Figure 5: Comparison of two motion images. Plot (A) is 15 km per day motion, plot (B) is 30 km per day. Note the textural similarities in the transition regions and the very flat response in the extremities.

REFERENCES

[1] A. R. Hosseinmostafa, V. I. Lytle, K. C. Jezek, S. P. Gogineni, S. F. Ackley, and R. K. Moore, "Comparison of radar backscatter from antarctic and arctic sea ice," *Journal of Electromagnetic Waves and Applications*, vol. 9, no. 3, pp. 421--438, 1995.

[2] P. Lecomte, A. Cavanie, and F. Gohin, "Recognition of sea ice zones using ERS-1 scatterometer data," in *Proceedings of IGARSS 93*, pp. 855--857, IEEE, 1993.

[3] D. Long and M. Drinkwater, "Greenland Ice Sheet Surface Properties Observed by the Seasat-A Scatterometer at Enhanced Resolution," *Journal of Glaciology*, vol. 40, pp. 213--230, 1994.

[4] D. Long, P. Hardin, and P. Whiting, "Resolution Enhancement of Spaceborne Scatterometer Data," *IEEE Transactions on Geoscience and Remote Sensing*, vol. 31, pp. 700--715, 1993.

[5] D. Daum, D. Long, and W. Davis, "Reconstructing Enhanced Resolution Images From Spaceborne Microwave Sensors," in *Proceedings of IGARSS 94*, pp. 2231--2233, IEEE, 1994.